Supporting Information

Steric Control and Mechanism of Benzaldehyde Oxidation by Polypyridyl Oxoiron(IV) Complexes: Aromatic versus Benzylic Hydroxylation of Aromatic Aldehydes

Ramona Turcas, Dóra Lakk-Bogáth, Gábor Speier, and József Kaizer*
Department of Chemistry, University of Pannonia, 8201 Veszprém, Hungary

Experimental

Materials and methods: All manipulations were performed under a pure argon atmosphere using standard Schlenk-type techniques unless otherwise stated. Solvents used for the reactions were purified by standard methods and stored under argon. Benzaldehyde derivatives were purchased from from Sigma-Aldrich. The ligands L_1 and L_2, and complexes **1** and **2** were prepared according to published procedures.[11a, 11b] Infrared spectra were recorded with an Avatar 330 FTIR Thermo Nicolet instrument. UV/Vis spectra were recorded with an Agilent 8453 diode-array spectrophotometer with quartz cells. Microanalyses were performed by the Microanalytical Service of the University of Pannonia and Atlantic Microlab.

$[Fe^{III}(asN4Py)(Salicylate)]ClO_4$ (5) was synthesized by reacting equimolar amounts of $[Fe^{II}(asN4Py)(O)]^{2+}$ **(3)** and salicylic acid in CH_3CN under O_2.

FT-IR (KBr, cm^{-1}): 1601 s, 1561 m, 1482 s, 1454 s, 1390 s, 1086 s, 912 w, 755 m, 621 m. UV–Vis (MeCN) λmax(log ε, $dm^3mol^{-1}cm^{-1}$): 568 (3.29). Anal. Calcd. for $C_{31}H_{27}ClFeN_5O_7$ (672.87): C, 55.33; H, 4.04; N, 10.41. Found C, 55.13; H, 4.12; N, 10.48.

Description of the benzaldehyde oxidation with Fe(IV) intermediates (2 and 4)

1 or **2** complex (1.5×10^{-3} M) was dissolved in acetonitrile (1.5 mL), then iodosylbenzene (3.00×10^{-3} M) was added to the solution. The mixture was stirred for 50 minutes then the excess iodosylbenzene was removed by filtration. Benzaldehyde was added to the solution and the reaction was monitored by UV-vis spectrophotometer (Agilent 8453) at 705 or 695 nm (λ = 400 M^{-1} cm^{-1}). The hydrolysed and methylated products were identified by GC (HP 4890D instrument with flame ionization detector equipped with an HP-5 capillary column, standard = naphtalene), and the yields were calculated based on the amount of oxidant (**2** or **4**) used in the reactions. The GC-MS (GCMS-QP2010 SE, Shimadzu) analysis of the residue, after treatment with ethereal diazomethane showed the presence of methyl-benzoate: m/z (%) = 136 (29) [M^+], 105 (100), 77(88) for **2**, and methyl-salicylate: m/z (%) = 152 (31) [M^+], 120 (100), 121 (27), 92 (89) for **4**.

*Corresponding author. Tel.: +36 88 62 4720; Fax: + 36 88 62 4469.
E-mail address: kaizer@almos.vein.hu.

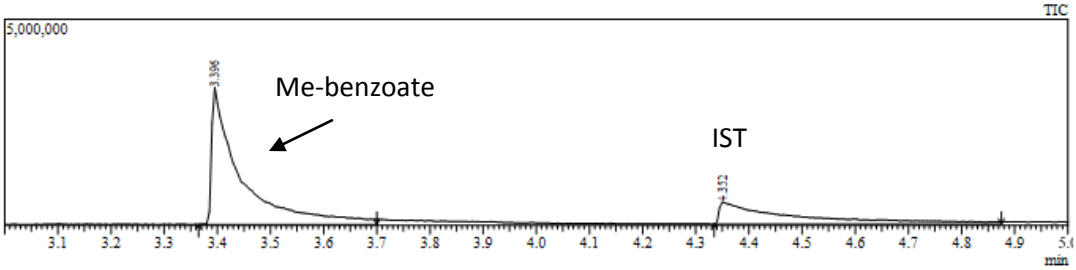

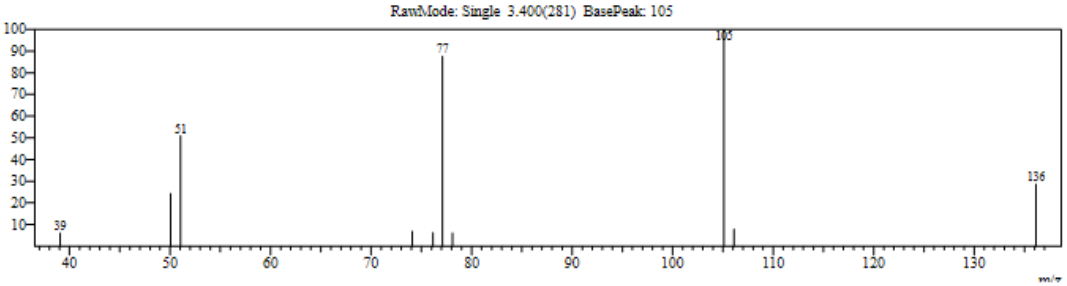

R.Time:3.400
RawMode: Single 3.400(281)
BasePeak: 105

Rel. Int.	m/z	Rel. Int.	m/z	Rel. Int.	m/z	Rel. Int.	m/z	Rel. Int.	m/z
6.2	39	51.0	51	6.3	76	6.2	78	7.9	106
24.3	50	7.0	74	87.6	77	100.0	105	28.7	136

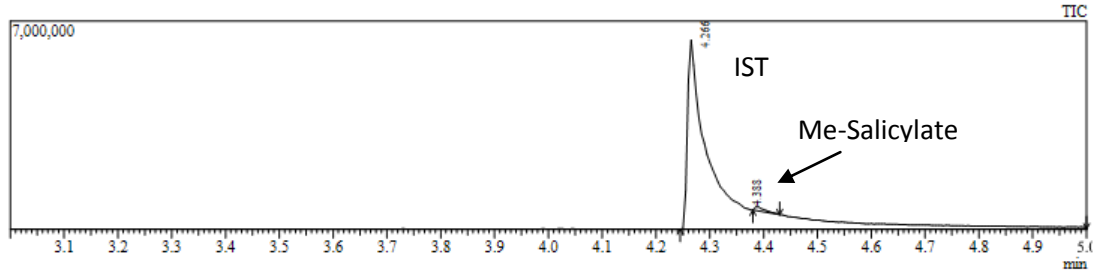

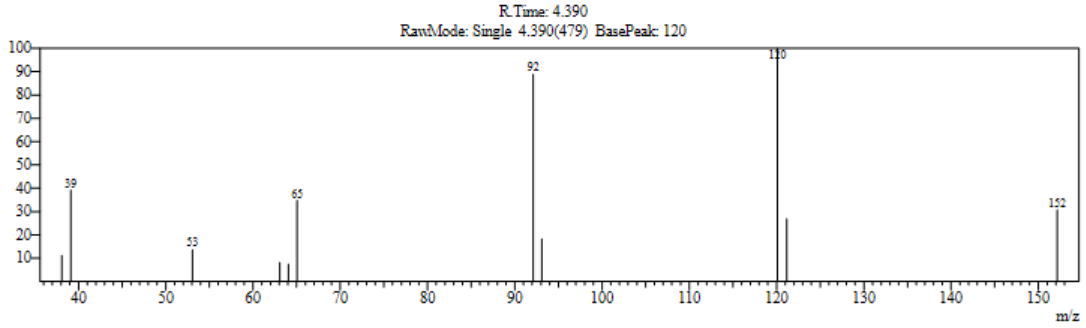

R.Time:4.390
RawMode: Single 4.390(479)
BasePeak: 120

Rel. Int.	m/z	Rel. Int.	m/z	Rel. Int.	m/z	Rel. Int.	m/z
11.1	38	8.1	63	88.8	92	26.9	121
39.1	39	7.4	64	18.2	93	30.6	152
13.6	53	34.8	65	100.0	120		

Table S1. Kinetic data for the hydroxylation reaction of benzaldehyde with $[Fe^{IV}(N4Py)(O)]^{2+}$ **(2)**.

N_0	T (K)	$[Fe]_0$ (10^{-3} M)	PhCHO (M)	k' ($10^{-2}s^{-1}$)	k_2 (10^{-2} $M^{-1}s^{-1}$)
1	298	1.5	0.2	1.71	8.55
2[a]	298	1.5	0.3	2.6	8.67
3	298	1.5	0.3	2.48	8.29
4	298	1.5	0.3	2.51	8.36
5	298	1.5	0.4	3.2	8.25
6	298	1.5	0.49	4.05	8.27
7	278	1.5	0.2	0.91	4.53
8	283	1.5	0.2	1.10	5.50
9	289	1.5	0.2	1.30	6.50
10	293	1.5	0.2	1.58	7.90
11	298	1.5	0.2	1.71	8.55
12	303	1.5	0.2	2.10	10.50

[a]under O_2.

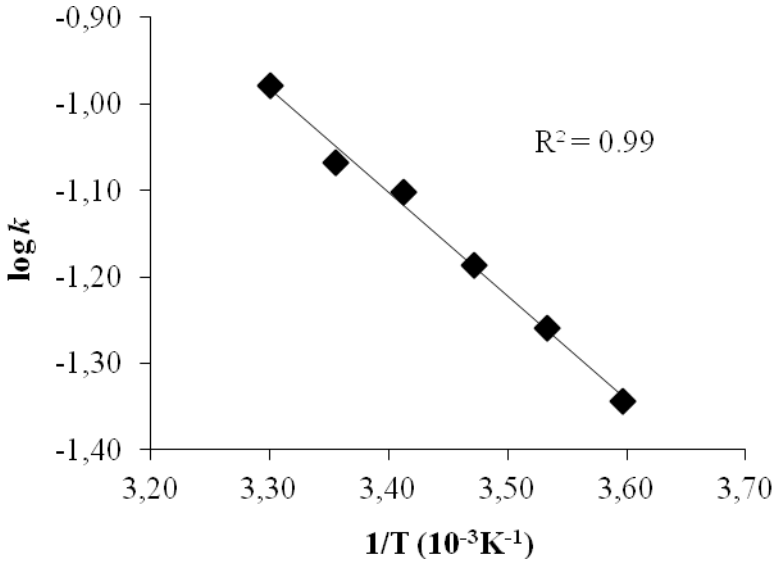

Fig. S1. Arrhenius plot of the hydroxylation reaction of benzaldehyde with $[Fe^{IV}(N4Py)(O)]^{2+}$ **(2)**.

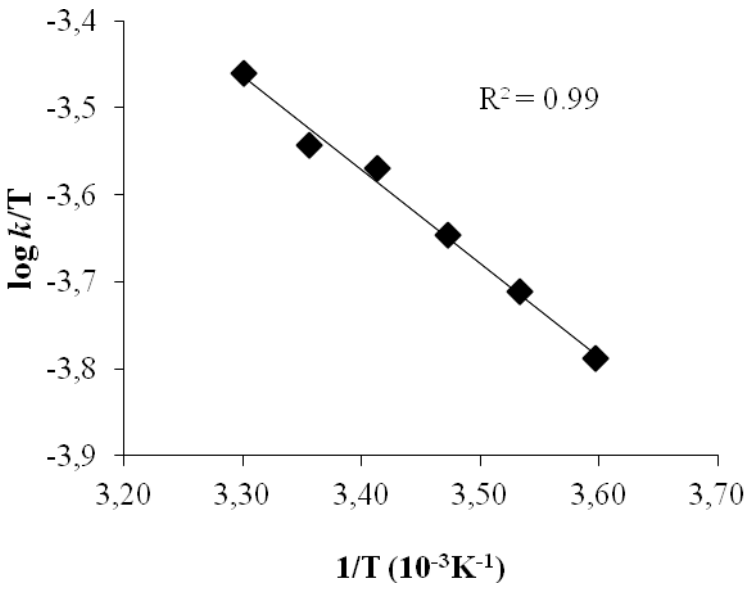

Fig. S2. Eyring plot of the hydroxylation reaction of benzaldehyde with $[Fe^{IV}(N4Py)(O)]^{2+}$ **(2)**.

Table S2. Hammett data for the hydroxylation reaction of benzaldehyde with $[Fe^{IV}(N4Py)(O)]^{2+}$ **(2)**.

N_0	T (K)	$[Fe]_0$ (10^{-3} M)	σ_p	PhCHO (M)	k' (10^{-3} s^{-1})	k_2 (10^{-2} $M^{-1}s^{-1}$)
1	298	1.5	0.23	Cl	3.98	3.98
2	298	1.5	0.66	CN	2.44	1.22
3	298	1.5	-0.17	CH_3	20.60	10.30
4	298	1.5	0	H	17.10	8.55
5	298	1.5	0.78	NO_2	0.71	0.71
6	298	1.5	-0.27	OCH_3	29.00	14.50

Table S3. Kinetic data for reactions of $[Fe^{IV}(N4Py)(O)]^{2+}$ (**2**) with PhCDO (*KIE*).

N_0	T (K)	$[Fe]_0$ (10^{-3} M)	PhCDO (M)	k' (10^{-2} s^{-1})	k_2 (10^{-2} $M^{-1}s^{-1}$)	KIE
1	298	1.5	0.2	0.077	0.39	26.5
2	298	1.5	0.3	0.079	0.26	
3	298	1.5	0.4	0.131	0.32	

Table S4. Kinetic data for the hydroxylation reaction of benzaldehyde with $[Fe^{IV}(asN4Py)(O)]^{2+}$ **(4)**.

N_0	T (K)	$[Fe]_0$ (10^{-3} M)	PhCHO (M)	k' (10^{-3} s^{-1})	k_2 (10^{-2} $M^{-1}s^{-1}$)
1	298	1.5	0.2	4.50	2.25
2	298	1.5	0.3	6.47	2.16
3[a]	298	1.5	0.3	6.81	2.27
4[b]	298	1.5	0.3	7.02	2.34
5	298	1.5	0.4	9.00	2.25
6	298	1.5	0.49	11.50	2.35
7	298	1.5	0.55	13.00	2.36
8	278	1.5	0.3	2.18	0.72
9	283	1.5	0.3	2.84	0.94
10	289	1.5	0.3	3.85	1.28
11	293	1.5	0.3	4.80	1.6
12	298	1.5	0.3	6.47	2.16
13	303	1.5	0.3	7.17	2.39

[a] Under air. [b] Under O_2.

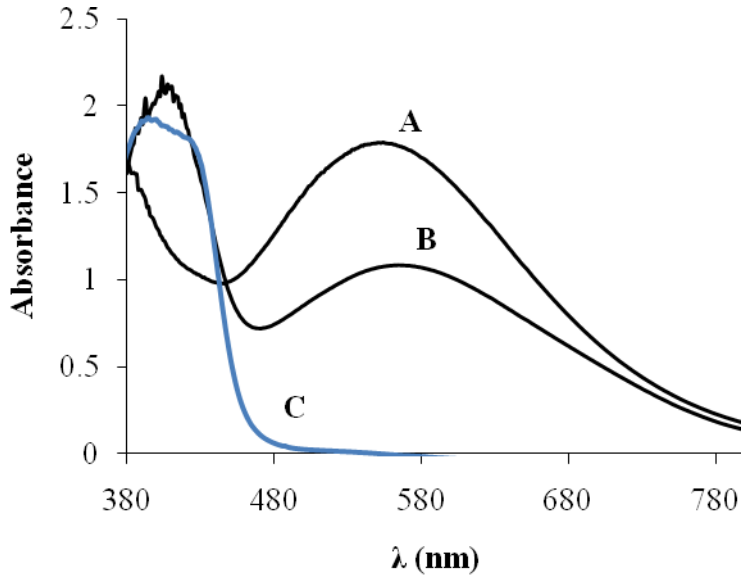

Fig. S3. UV-vis spectrum of the complex **$[Fe^{III}(asN4Py)(Salicylate)]ClO_4$ (5)** synthesized by reacting equimolar amounts of $[Fe^{II}(asN4Py)(O)]^{2+}$ **(3)** (1 mM) and salicylic acid in CH_3CN under O_2, (A), its maximum formation (~50%) in the presence of large excess of benzaldehyde and **4** (1 mM) (B), and the UV-vis spectrum of **3** (0.2 mM) (C).

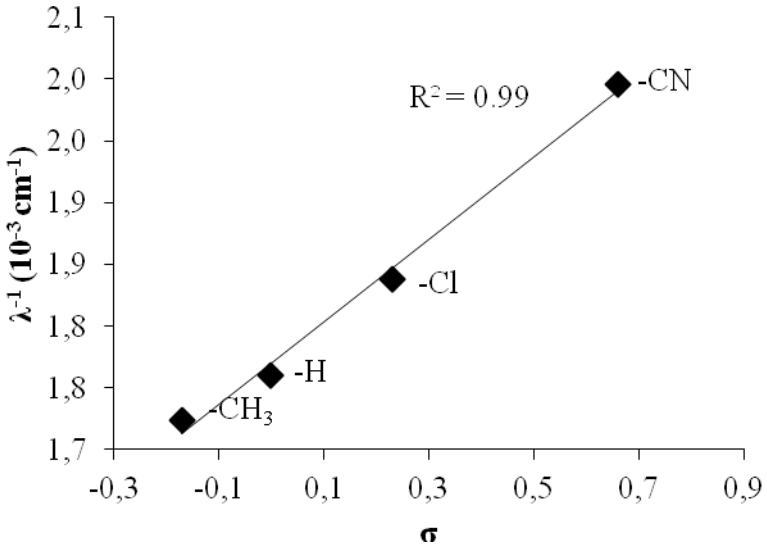

Fig. S4. Correlation between LMCT bands (λ^{-1}) versus Hammett σ values for the salicylato-iron(III) complexes formed in the hydroxylation reactions of benzaldehydes with $[Fe^{IV}(asN4Py)(O)]^{2+}$ **(4)**.

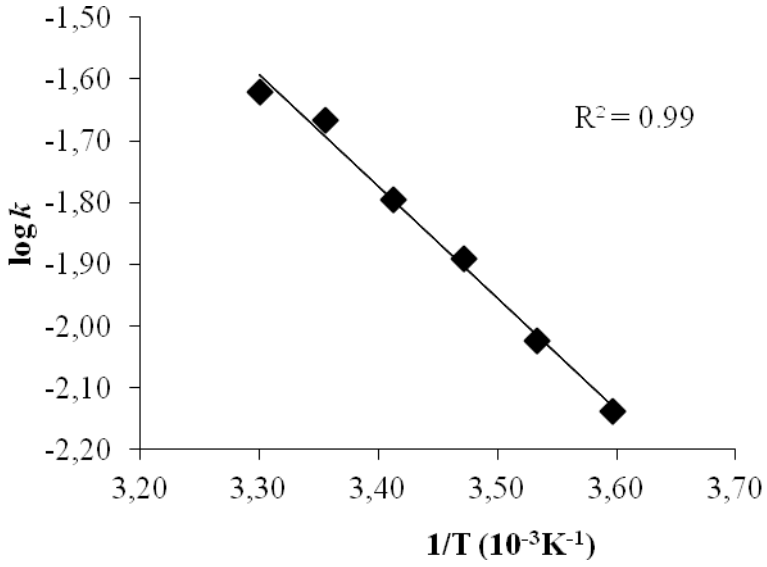

Fig. S5. Arrhenius plot of the hydroxylation reaction of benzaldehyde with $[Fe^{IV}(asN4Py)(O)]^{2+}$ **(4)**.

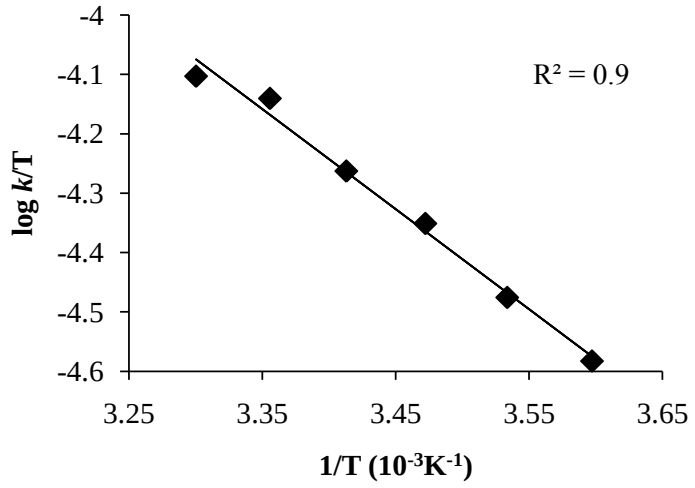

Fig. S6. Eyring plot of the hydroxylation reaction of benzaldehyde with $[Fe^{IV}(N4Py)(O)]^{2+}$ **(4)**.

Table S5. Hammett data for the hydroxylation reaction of benzaldehyde with $[Fe^{IV}(asN4Py)(O)]^{2+}$ **(4)**.

N_0	T (K)	$[Fe]_0$ (10^{-3} M)	σ_p	PhCHO (M)	k' (10^{-4} s^{-1})	k_2 (10^{-3} $M^{-1}s^{-1}$)
1	298	1.5	0.23	-Cl	8.23	8.23
2	298	1.5	0.66	-CN	3.50	1.17
3	298	1.5	-0.17	$-CH_3$	160.00	53.33
4	298	1.5	0	-H	64.70	21.60

Table S6. Kinetic data for reactions of $[Fe^{IV}(asN4Py)(O)]^{2+}$ (**2**) with C_6D_5CHO (*KIE*).

N_0	T (K)	$[Fe]_0$ (10^{-3} M)	deu-PhCHO (M)	k' (10^{-3} s^{-1})	k_2 ($10^{-2}M^{-1}s^{-1}$)	*KIE*
1	298	1.5	0.3	1.5	0.5	3.69
2	298	1.5	0.4	2.5	0.62	
3	298	1.5	0.55	3.2	0.58	

Table S7. Kinetic data for reactions of $[Fe^{IV}(asN4Py)(O)]^{2+}$ (**2**) with PhCDO (*KIE*).

N_0	T (K)	$[Fe]_0$ (10^{-3} M)	deu-PhCHO (M)	k' (10^{-3} s^{-1})	k_2 ($10^{-3}M^{-1}s^{-1}$)	*KIE*
1	298	1.5	0.6	0.32	0.53	36.79
2	298	1.5	0.9	0.57	0.63	
3	298	1.5	1.2	0.69	0.57	